Weak Localization of Light in a Disordered Microcavity

M. Gurioli,[1,2,†] F. Bogani,[3] L. Cavigli,[2] H. Gibbs,[4] G. Khitrova,[4] and D. S. Wiersma[2,‡]

[1]*Dipartimento di Fisica, Universitá di Firenze, I-50019 Sesto-Fiorentino (FI), Italy*

[2]*INFM-MATIS and European Laboratory for Non-linear Spectroscopy, Sesto Fiorentino (Florence), Italy**

[3]*Dipartimento di Energetica, Universitá di Firenze, I-50134-Firenze (FI), Italy*

[4]*Optical Sciences Center, University of Arizona, Tucson, Arizona 85721, USA*

(Received 25 May 2004; published 10 May 2005)

We report the observation of weak localization of light in a semiconductor microcavity. The intrinsic disorder in a microcavity leads to multiple scattering and hence to static speckle. We show that averaging over realizations of the disorder reveals a coherent backscattering cone that has a coherent enhancement factor ≥ 2, as required by reciprocity. The coherent backscattering cone is observed along a ring-shaped pattern due to confinement by the microcavity.

DOI: 10.1103/PhysRevLett.94.183901 PACS numbers: 42.25.Dd, 42.25.Hz, 78.67.Pt

The behavior of light waves in complex dielectric systems is full of surprises. Complex dielectrics are structures in which the dielectric constant varies on length scales that are roughly comparable to the wavelength of light. If this variation is periodic a photonic crystal is formed. In disordered dielectric structures, on the other hand, light waves undergo a complicated multiple scattering process. Interference effects can survive random multiple light scattering and lead to interesting phenomena like speckle correlations, universal conductance fluctuations of light, and optical Anderson localization [1]. The most robust of interference phenomena is weak localization [2] which originates from the fundamental concept of reciprocity and is observable as a coherent enhancement of the intensity in and around the backscattering direction. This enhancement is called the cone of coherent backscattering. Since the first experimental observation of coherent backscattering from colloidal suspensions [2], the phenomenon has been successfully studied in various random materials like powders [3–5], photonic crystals [6], cold atom gases [7], and liquid crystals [8]. A fundamental property of the coherent backscattering effect is that the intensity enhancement in the exact backscattering direction is exactly two. This is a direct consequence of the interference between reciprocal light paths. This enhancement factor can be reduced due to single scattering, incoherent processes, and Anderson localization effects [5]. The concepts of weak and strong (i.e., Anderson) localization have originally been introduced in the study of electronic transport in metals where they are related to the metal-insulator transition.

Much less is known about multiple light scattering in confined semiconductor systems like semiconductor microcavities. Often microcavities are optimized for minimum disorder and hence minimum light scattering. However, optimizing a microcavity for strong scattering should allow to study the fascinating interplay between multiple scattering transport phenomena like weak and strong localization and strong optical cavity confinement. It is known that single scattering from microcavities can have an important elastic component [9–16] and multiple scattering processes can indeed be observed [16]. Microscopic theories often neglect multiple scattering processes [11,12], however the possibility of observing weak localization of microcavity polaritons has been very recently proposed [17]. Enhanced backscattering from quantum well excitons has been studied as well, in which case the localized character of the excitonic wave function could be observed close to resonance [18,19].

There has been a recent backscattering study on semiconductor microcavities [10], in which the intensity at exact backscattering was reported to be 10 times the diffuse background. In this pioneering study a single realization of the disorder was used, which does not allow for the observation of coherent backscattering [3,4]. To observe coherent backscattering requires performing an ensemble average over realizations of the disorder, otherwise the backscattered signal is completely dominated by speckle fluctuations which can be orders of magnitude larger then the coherent backscattering cone [3,4].

In this Letter we report the observation of weak localization from a semiconductor microcavity. We show that by averaging over a large number of realizations of the disorder one obtains a coherent backscattering effect with coherent enhancement ≤ 2, consistent with theory. This observation allowed us to determine also the width of the backscattering cone and estimate the transport mean free path. We find that the width depends only mildly on detuning of the frequency with respect to the polariton resonance.

We investigated a semiconductor microcavity (CAT13) consisting of a 14 multilayer GaAs/AlAs mirror, a wedged λ GaAs spacer containing a single 8.5 nm $In_{0.04}Ga_{0.96}As$ quantum well, and another 16.5 multilayer GaAs/AlAs mirror. Standard reflectivity as well as spatially resolved imaging measurements [14] were used to characterize the polariton anticrossing curve. We find a Rabi splitting with energy difference $\Omega = 3.3$ meV at resonance. The wedge angle of the sample $\beta \approx 7$ μrad corresponds to a gradient of $r = 11.6$ meV/mm. In the following we will describe the resonance condition by using the energy difference $\delta = E_{\mathrm{cav}} - E_{\mathrm{exc}}$ with E_{cav} the energy of the bare cavity mode and E_{exc} the energy of the exciton mode. The polariton linewidth at $\delta = 0$ is about 0.7 meV. A study of the spectral components of the resonant secondary emission of this sample, including the interplay between the elastic resonant Rayleigh scattering (RRS) and the inelastic photoluminescence components, can be found elsewhere [14,15]. This study shows that elastic scattering (resonant Rayleigh scattering) largely dominates over (incoherent) photoluminescence in the lower polariton branch and that the major source of the scattering is the dielectric disorder inside the cavity and its Bragg mirrors. Therefore, to optimize the elastic multiple scattering component we concentrate on negative detuning (lower polariton branch).

To study the angular distribution of the backscattered light from this sample we used a conventional coherent backscattering measurement scheme [5]. The output of a single mode Ti:sapphire laser (0.5 W, 831.6 nm at $\delta = 0$) was spatially filtered and collimated into an 3 mm diameter beam and focused through a beam splitter onto the sample. The laser beam was focused to a spot of about 40 μm diameter, which turned out to give the best coupling of the light into our microcavity [14]. The sample was contained in a standard vacuum chamber and maintained at a temperature of 8 K. The sample normal was tilted under an angle $\alpha = 7°$ with respect to the incoming laser beam to separate the direct reflection of the sample surface from the exact backscattering direction. The backscattered light was monitored by a cooled CCD camera.

Typical images of the backscattered light are reported in Fig. 1. Results are shown for two different points on the sample, maintaining the same detuning, $\delta = -2$ meV. Hence Figs. 1(a) and 1(b) correspond to two realizations of the disorder, at otherwise the same parameters. The elastically scattered light is distributed in a ring-shaped pattern. This is typical for Rayleigh scattering from microcavities which is confined in a cone due to the condition of conservation of the modulus of the in-plane wave vector $k_{\parallel}$ [9]. The center of the ring indicates the direction of the normal to the sample surface and its radius is $2\pi \sin(\alpha)/\lambda$ with λ the vacuum wavelength of light and α the incidence angle. The arrows indicate the direction of the direct reflection of the sample surface and the backscattering (BS) direction. A neutral density filter is placed in the direct reflection of the laser to avoid over exposure of the CCD camera. This gives rise to the dark square around the laser spot. In addition, we observe two very bright perpendicular lines which correspond to the directions of the two crystallographic axes [110] and $[\bar{1}10]$, consistent with previous observations [10,16]. (See also Fig. 2.) This indicates that the scattering in these samples is highly anisotropic along their crystallographic axes and can be attributed partially to interfacial misfit dislocations due to the lattice mismatch of the AlAs layers in the cavity Bragg mirrors [14,15]. We observe that the stripes indeed rotate if the sample is rotated in its plane. The sample angle was chosen so the stripes lie along the ring of multiple scattering, thereby keeping them away from the backscattering direction. We have verified that results reported hereafter do not depend on the exact choice of this angle. For better visibility, the intensity in the right part of both Figs. 1(a) and 1(b) has been multiplied by a scale factor of 5.

The grainy pattern observed in Fig. 1 is speckle, which is known to occur due to interference in multiple scattering [3,4]. Comparison of Figs. 1(a) and 1(b) clearly shows that the speckle pattern changes completely for different realizations of the disorder. In particular, Fig. 1(b) shows a bright speckle spot exactly in the backscattering direction, which is not observed in Fig. 1(a). This illustrates why averaging over realizations of the disorder is vital when

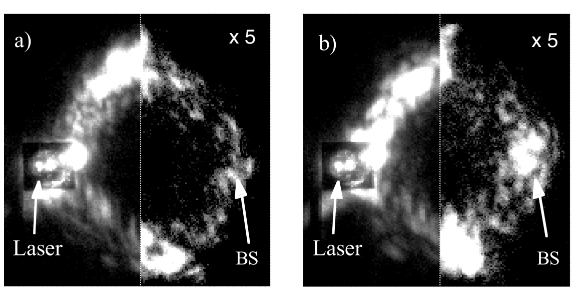

FIG. 1. Backscattered radiation pattern from our semiconductor microcavity at detuning $\delta = -2$ meV for two different points on the sample. The intensity in the right half of both figures has been multiplied by a factor of 5 for better visibility. The center of the ring corresponds to the direction of the normal incidence to the sample; the directions of specular reflection and backscattering are indicated by arrows. The grainy pattern in both pictures is due to speckle.

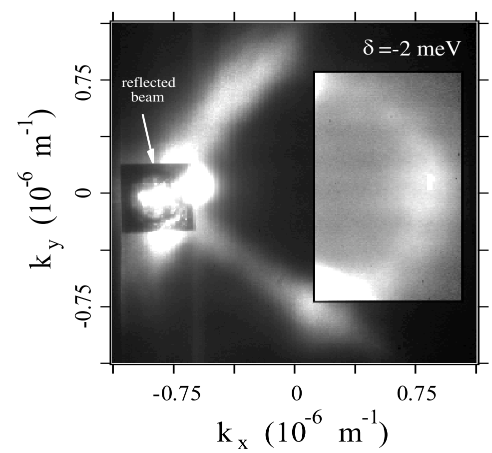

FIG. 2. Ensemble averaged backscattered radiation pattern. ($\delta = -2$ meV.) The region around the backscattering direction has been amplified by a factor of 5 for better visibility. Note the enhancement of intensity in the backscattering direction.

studying coherent backscattering from solid samples. In random samples based on, e.g., suspensions of microspheres, this ensemble average is conveniently obtained by the Brownian motion of the microspheres [2]. For a solid sample, ensemble averaging can be achieved by accumulating several backscattering images from independent positions on the sample and averaging them. In practice, we have obtained the required averaging by recording over 100 independent backscattering patterns as in Fig. 1 from different points on the sample. This was done by moving the sample along its plane and in the direction perpendicular to the cavity gradient. The cavity detuning in each measurement was carefully checked by monitoring the reflection spot [20].

The resulting averaged backscattering signal is reported in Fig. 2 for the case $\delta = -2$ meV. In the ensemble averaged signal one can clearly observe the presence of the ring of scattered light with an enhancement of the intensity around the exact backscattering direction. Coherent backscattering is usually described in terms of the scattering angle θ, defined as the angle between incoming and outgoing wave vectors. In the case of coherent backscattering from a microcavity the light is confined to a ring shaped pattern due to the condition of conservation of the modulus of the in-plane wave vector $k_{\|}$:

$$|\vec{k}_i| \sin\alpha = |\vec{k}_{\|}| = |\vec{k}_f| \sin\alpha, \tag{1}$$

with $\vec{k}_i$ and $\vec{k}_f$ the incoming and outgoing wave vectors, α the incidence angle with respect to the sample normal, and $\vec{k}_{\|}$ the wave vector of the cavity polariton inside the sample. The scattering angle θ relates to the azimuth angle ψ along the ring as

$$\sin(\theta/2) = \sin(\psi/2)\sin(\alpha), \tag{2}$$

where ψ and θ are taken zero at exact backscattering. (See also Fig. 3 which shows a sketch of the angular geometry used in the experiment.)

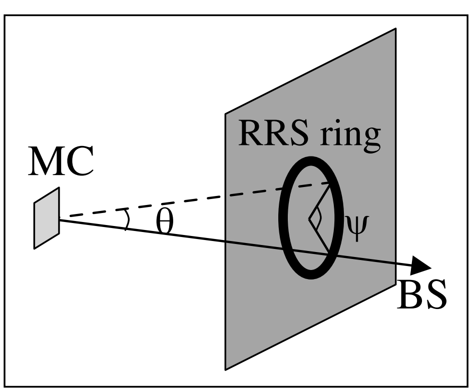

FIG. 3. Sketch of the angular geometry used in our experiment. BS indicates the exact backscattering direction $\theta = \phi = 0$, and MC indicates the microcavity.

In Fig. 4, the backscattered intensity is plotted as a function of the angle θ for two different cavity detunings. The coherent enhancement at backscattering is between 1.5 and 1.6, consistent with the requirement that the enhancement factor should be lower than two. The observed value is typical for experiments with linear polarized light [2,4,5]. The noise is mainly due to residual speckle, since our ensemble average can be taken only over a limited number of realizations.

The physical picture of the random walk process in our system is the following. The incoming beam enters the sample under an angle α and launches a polariton inside the sample with a wave vector that is equal to the parallel component of the incoming wave vector. The polariton then performs a two-dimensional random walk inside the microcavity until it is coupled out again. The modulus of the in-plane wave vector is conserved, which means the outgoing wave vector makes again the same angle α with the sample normal, thereby confining the outgoing light to a ring shaped distribution.

Although there is no exact theory available for weak localization in a semiconductor microcavity, one can still draw some conclusions from the experimental observations that are of general validity. The angular width W of

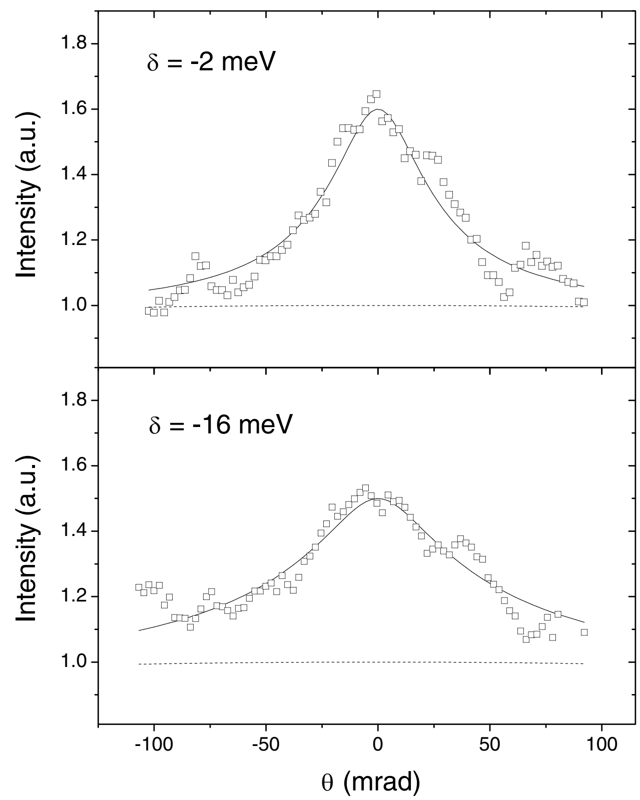

FIG. 4. Measured angular dependence of the intensity calculated from the angular dependence along the ring of multiple scattering. (a) Top panel: $\delta = -2$ meV; (b) Bottom panel: $\delta = -16$ meV. The solid line is obtained from a regular diffusion model of coherent backscattering [21].

the backscattering cone (measured at full width at half maximum) is directly related to the average distance d between the first and last scattering event:

$$W \simeq a(kd)^{-1}, \tag{3}$$

with k the modulus of the wave vector and a a numerical prefactor of order 1. This relation is independent of the specific random system under study and the nature of the multiple scattering process. If one measures the angular width W outside the sample using θ as in Fig. 4, one has to use the vacuum value of k in this equation. Alternatively one can measure the angular width of the cone along ψ, which is the angle of the scattered polariton in the plane of the sample. In that case Eq. (3) remains valid if one uses the internal wave vector $k = |\vec{k}_{\parallel}| = |\vec{k}_f| \sin\alpha$.

The distance d between the first and last scattering event depends linearly on the transport mean free path ℓ, defined as the average distance over which the polariton loses its memory of propagation direction. The value of a depends on the statistics of the disorder. For Gaussian disorder in a three-dimensional system Eq. (3) can be written as $W = 0.7(k\ell)^{-1}$. For diffusion in a two-dimensional system the angular width of the backscattering cone is expected to be very close to this value. If we apply this to our measurements, as was done in Ref. [10], we obtain $k\ell = 12.3(\pm 20\%)$ at $\delta = -2$ meV and $k\ell = 7.4(\pm 20\%)$ at $\delta = -16$ meV when the polariton becomes photonlike.

It is possible to compare the backscattering cone as measured from the microcavity with the theoretical line shape of coherent backscattering in regular diffusive systems. Although, *a priori*, there is no reason why the backscattering cone from a microcavity should match this classical line shape, the comparison is instructive since it gives an insight in the path length distribution in the microcavity. Independently from the nature of scattering and the geometry of the system under study, the shape of the backscattering cone is the Fourier transform of the distance distribution on the sample interface between incoming and outgoing light waves. This result holds also for a complex system such as a microcavity with disorder. We calculated this theoretical line shape using the approach of Ref. [21] and have plotted the result in Fig. 4 as a solid line. The correspondence between theoretical and experimental curves indicates that the path length distribution inside the microcavity is similar to that of a regular diffusive system with Gaussian disorder.

In conclusion we have observed weak localization of light from a semiconductor microcavity in the form of a cone of coherent backscattering, obtained by performing an ensemble average over realizations of the disorder. A microcavity with disorder constitutes a system in the intermediate regime between fully ordered systems like photonic crystals and disordered systems like powders. The 2D character of the random walk inside the cavity is expected to facilitate Anderson localization effects. Theoretical predictions show that in the Anderson localized regime, the coherent backscattering cone remains visible and of finite width [22]. Future studies could involve systems with increased disorder to study the interplay between microcavity confinement and Anderson localization.

Work at LENS is supported by the European Commission, by EU MRTN-CT-2003-503677, by MIUR Cofin 2002 and 2004, and by the INFM project Photonic. The Tucson group acknowledges support from NSF AMOP and NSF EPDT.

*Electronic address: www.lens.unifi.it
Electronic address: www.complexphotonics.org
†Electronic address: gurioli@lens.unifi.it
‡Electronic address: wiersma@lens.unifi.it

[1] *Photonic Crystals and Light Localization in the 21st Century*, edited by Costas M. Soukoulis, Nato Science Series C 563 (Kluwer, Dordrecht, 2000).
[2] Y. Kuga and A. Ishimaru, J. Opt. Soc. Am. A **1**, 831 (1984); M. Van Albada and A. Lagendijk, Phys. Rev. Lett. **55**, 2692 (1985); P. Wolf and G. Maret, Phys. Rev. Lett. **55**, 2696 (1985).
[3] S. Etemad, R. Thompson, and M. J. Andrejco, Phys. Rev. Lett. **57**, 575 (1986).
[4] M. Kaveh *et al.*, Phys. Rev. Lett. **57**, 2049 (1986).
[5] D. S. Wiersma *et al.*, Phys. Rev. Lett. **74**, 4193 (1995).
[6] A. F. Koenderink *et al.*, Phys. Lett. A **268**, 104 (2000); J. Huang *et al.*, Phys. Rev. Lett. **86**, 4815 (2001).
[7] G. Labeyrie *et al.*, Phys. Rev. Lett. **83**, 5266 (1999); Y. Bidel *et al.*, Phys. Rev. Lett. **88**, 203902 (2002).
[8] D. V. Vlasov *et al.*, Pis'ma Zh. Eksp. Teor. Fiz. **48**, 86 (1988) [JETP Lett. **48**, 91 (1988)]; R. Sapienza *et al.*, Phys. Rev. Lett. **92**, 033903 (2004).
[9] T. Freixanet *et al.*, Phys. Rev. B **60**, R8509 (1999).
[10] R. Houdré *et al.*, Phys. Rev. B **61**, R13 333 (2000).
[11] D. M. Whittaker, Phys. Rev. B **61**, R2433 (2000).
[12] A. V. Shchegrov *et al.*, Phys. Rev. Lett. **84**, 3478 (2000).
[13] G. Cassabois *et al.*, Phys. Rev. B **64**, 45 321 (2001).
[14] M. Gurioli *et al.*, Phys. Rev. B **64**, 165309 (2001).
[15] M. Gurioli *et al.*, Phys. Status Solidi A **190**, 363 (2002).
[16] W. Langbein and J. M. Hvam, Phys. Rev. Lett. **88**, 047401 (2002).
[17] M. Litinskaia, G. C. La Rocca, and V. M. Agranovich, Phys. Rev. B **64**, 165316 (2001).
[18] V. Savona, E. Runge, and R. Zimmermann, Phys. Rev. B **62**, R4805 (2000).
[19] W. Langbein *et al.*, Phys. Rev. Lett. **89**, 157401 (2002).
[20] A narrow dark fringe can be observed in the reflection spot that is very sensitive to the exact value of the detuning and which can be conveniently used to monitor the detuning when the sample is moved to a new position [10,14].
[21] M. B. van der Mark, M. P. van Albada, and A. Lagendijk, Phys. Rev. B **37**, 3575 (1988).
[22] B. van Tiggelen, A. Lagendijk, and D. S. Wiersma, Phys. Rev. Lett. **84**, 4333 (2000).